CrystEngComm

Accepted Manuscript

ROYAL SOCIETY OF CHEMISTRY

www.rsc.org/crystengcomm

Effect of composition deviation on microstructure and luminescence property of Nd:YAG ceramics

Haiming Qin [a,b], Jun Jiang [a], Haochuan Jiang [a], Yuanhua Sang [b], Dehui Sun [b], Xinhai Zhang [c]*, Jiyang Wang [b], Hong Liu [b]*

[a] Ningbo Institute of Materials Technology and Engineering, Chinese Academy of Sciences, Ningbo, 315201, China

[b] State Key Laboratory of Crystal Materials, Shandong University, Jinan, 250100, China

[c] Department of Electrical and Electronic Engineering, South University of Science and Technology of China, Shenzhen, 518055, China

***Corresponding authors**

Hong Liu, Email: hongliu@sdu.edu.cn Tel.: +86-531-88362807; Fax: +86-531-88362807

Xinhai Zhang, Email: zhang.xh@sustc.edu.cn Tel.: +86-755-88018566

Abstract

Neodymium-doped yttrium aluminum garnet (Nd:YAG) ceramics with different Al_2O_3/Y_2O_3 deviation levels were prepared *via* a solid state reaction-vacuum sintering method. Transparent ceramics were obtained with its composition in between stoichiometric Nd:YAG $Y_{2.97}Nd_{0.03}Al_5O_{12}$ and 2% Y_2O_3 excessive Nd:YAG $Y_{2.97}Nd_{0.03}Al_5O_{12}\cdot 2\%Y_2O_3$. Stoichiometric Nd:YAG ceramic obtains homogeneous grain microstructure and clean grain boundaries. Nonstoichiometric composition lead to different ceramic microstructures from that of the stoichiometric Nd:YAG. Nanograins of excessive Al_2O_3 remain inside the Nd:YAG grains in Al_2O_3-excess ceramics, while the Y-rich compounds recrystallize at the Nd:YAG grain boundaries in Y_2O_3-excess ceramics. Photoluminescence spectra of sintered ceramics around 808 nm and 1064 nm were also studied. Peak positions of their luminescent spectra are little affected by composition deviation while their intensity is evidently declined due to existence of second phase arise by composition deviation. Results of this work can contribute to the controllable synthesis of highly transparent YAG ceramics and further exploration of the Nd ion spectra.

Introduction

Yttrium aluminum garnet (YAG) material is attractive as matrix of laser medium and luminescent material due to its excellent chemical and physical properties[1-8].

YAG single crystal has several favorable properties such as the physical, chemical stability, and transparency over a broad spectral range. Neodymium (Nd) ion is the most widely used active ion in laser gain medium for its appropriate four level system and low-threshold for laser oscillation. However, homogeneous doping of Nd ions over 1 at% as active ions in YAG single crystal is difficult [9] because of the low segregation coefficient of elemental Nd in YAG (about 0.2). Besides, the growth of neodymium-doped yttrium aluminum garnet (Nd:YAG) single crystal with the Czochralski method has many drawbacks, such as its low growth rate and expensive equipment needed. Commercial Nd:YAG single crystals are grown at approximately 2000 ^{o}C for a growth period about 1000-2000 hours [10]. At the same time, the core in the central region of the single crystal ingot and facets arised from the central region to the outer region limit the ultilization efficiency of single crystals. Only outer part of the ingot is suitable for laser medium application, which makes it hard to get large size device, and thus limits its application in high powder laser. Fortunately, with the technique development of the transparent ceramics, transparent YAG ceramic became a promising substitution of its single crystal [2-4]. Since the first demonstration of Nd:YAG ceramic laser by Ikesue *et al*. in 1995 [8], significant progress in preparing transparent YAG ceramics has been made. T Yanagitani and his coworkers reported a vacuum sintering method to fabricate highly transparent YAG ceramic laser material in 1999. In that process, the raw materials were prepared by nanotechnology. Laser performance of ceramics was thereby comparable to that of single crystals from then on. [5,7]

Different from single crystal growth process, ceramic is prepared *via* the atom diffusion among different particles during sintering process. Removal of impurities in ceramic preparation process is more difficult than that in single crystal growth process. As well known, the impurity phase in Nd:YAG can evidently affect the luminescent property, so it is essential to understand the effect of composition deviation on the microstructure and luminescent properties of Nd:YAG ceramics. Isao Sakaguchi *et al*. analyzed the effect of composition on the oxygen diffusion in YAG ceramics in 1996

[11]. They found that the diffusion of the oxygen at grain boundaries was suppressed in the Y_2O_3-excess specimen compared to the Al_2O_3-excess specimen. Akio Ikesue *et al*. studied the effect of Nd concentration on optical characteristics of Nd:YAG ceramic [12]. The Nd:YAG ceramics with Nd concentrations of 0.3–4.8 at% exhibited nearly the same fluorescence spectra as the Nd:YAG single crystal. The average grain size of the specimens decreased as the Nd doping concentration increased. However, systematic investigation on how Al_2O_3/Y_2O_3 composition deviation influents the microstructure and luminescence properties of Nd:YAG ceramics has not yet been reported. In present work, ceramics with different excessive amount of Y_2O_3 and Al_2O_3 were prepared *via* the solid state reaction-vacuum sintering method. Nano-sized Al_2O_3 grains are observed in the matrix grains of the Al_2O_3-excess ceramics, while Y-rich particles ($YAlO_3$, $Y_4Al_2O_9$) are noticed at the grain boundaries of the Y_2O_3-excess ceramics. According to photoluminescence (PL) characterization, spectra of Nd ion around 808 nm and 1064 nm are found to be little affected by composition deviation. However, their intensity is evidently varied due to the existence of second phase. Description and explanation to the microstructure evolution of YAG ceramics with composition deviation will be important for the further investigation on the existence and precipitation mechanism of second phases in garnet ceramics. On the other hand, result presented in this work can offer method to mediate ceramic microstructures according to designed composition deviation. That can contribute to the controllable synthesis of highly transparent garnet ceramics and microstructure control of ceramic based composite materials. What is more important, accurate mediation on the microstructure evolution of garnet ceramics can offer us effective approach to analyze the multi-site defects of active ions and energy transfer process among different phases. In depth understanding on the photoelectric processes in ceramics can be expected based on the work of this paper.

Experimental procedure

Nd:YAG ceramics were obtained *via* the solid state reaction-vacuum sintering

method. Briefly, α-Al_2O_3 (99.99%), Y_2O_3 (99.99%), and Nd_2O_3 (99.99%) were used as starting materials. Powders were blended according to the designed stoichiometric ratio of YAG with 1.0 at% Nd dopants. The blended powders were ball milled with high-purity corundum balls for 10 h in ethanol, with 0.5 wt% tetraethyl orthosilicate (TEOS) added as sintering aid. Then, the ethanol solvent was removed by drying the milled slurry at 80 ^oC for 24 h in oven. The dried mixture was grounded and sieved through 200-mesh screen. After being pressed with low pressure into Φ 13.2 mm pellets in a steel mold and then cold isostatically pressed at 250 MPa, the specimens were sintered at 1780 ^oC in vacuum (1.0×10^{-5} Pa) for up to 4 h in a tungsten mesh-heated vacuum furnace (712T, Thermal Technology LLC, USA). The heating rate was 5 ^oC/min, and the cooling rate was 10 ^oC/min. Several parallel samples with different Y/Al ratios including $Y_{2.97}Nd_{0.03}Al_5O_{12}$·1.5% Al_2O_3 (Formula means a Nd:YAG sample with 1.5 at% Al_2O_3 in excess, which is abbreviated as Al-1.5%.), $Y_{2.97}Nd_{0.03}Al_5O_{12}$ · 1.0% Al_2O_3 (Al-1.0%), $Y_{2.97}Nd_{0.03}Al_5O_{12}$ · 0.5% Al_2O_3 (Al-0.5%), $Y_{2.97}Nd_{0.03}Al_5O_{12}$ (Stoichiometric Nd:YAG), $Y_{2.97}Nd_{0.03}Al_5O_{12}$ · 1.0% Y_2O_3 (Y-1.0%), $Y_{2.97}Nd_{0.03}Al_5O_{12}$ · 2.0% Y_2O_3 (Y-2.0%), $Y_{2.97}Nd_{0.03}Al_5O_{12}$ · 3.0% Y_2O_3 (Y-3.0%), $Y_{2.97}Nd_{0.03}Al_5O_{12}$ · 4.0% Y_2O_3 (Y-4.0%) were prepared accordingly. Ball milling process is of an important procedure that affects the microstructure evolution and optical transparency of Nd:YAG ceramics. All preparation parameters we adopted locate around the optimum parameters reported in recent published paper about the preparation of Nd:YAG ceramics[22].

Selected sintered samples (Al-1.5%, Stoichiometric Nd:YAG, Y-3.0%) was sent for inductively coupled plasma (ICP, IRIS Intrepid II XSP) characterization. Micrographs of the ceramics were characterized using a field emission scanning electron microscopy (FESEM, S-4800, Japan) and a high resolution transmission electron microscopy (HRTEM, JEOL JEM 2100F, Japan). Phase compositions of the samples were measured by X-ray diffractometer (XRD, Advance D8, Germany). The ceramics with dimension 4 mm×4 mm×1 mm were polished on both sides (4 mm×4 mm) for transmittance measurement in the wavelength range of 200–1200 nm, using a

spectrophotometer (U-3500, Hitachi, Tokyo). PL spectra and time resolved spectra of the ceramics were recorded by a home-built PL spectroscopy apparatus. He-Cd laser with wavelength of 325 nm was used as the excitation light source.

Result and discussion

Figure 1 shows pictures of the as-sintered samples with different composition before and after annealing. Before annealing (see Figure 1a), Al_2O_3-excess samples feature red in color and low transmittance. Transparent ceramics were obtained with its composition in between stoichiometric Nd:YAG and Y-2%. Transmittance of the ceramics declines with the increase of Y_2O_3 in excess and becomes almost opaque when excessive Y_2O_3 is over 3%. Transmittance of the ceramics also declines with the increase of Al_2O_3 in excess. Meanwhile, the red color of the ceramics can be faded by annealing in oxygen atmosphere (see Figure 1b). Ceramics with composition in between stoichiometric Nd:YAG and Y-2% obtain better transparency after the annealing treatment while samples with more Y_2O_3 in excess show little improvement.

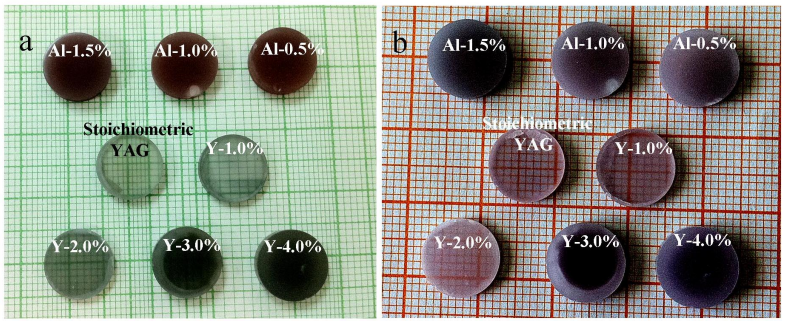

Figure 1. Pictures of sintered Nd:YAG samples with different composition (a) before annealing, (b) after annealing.

Figure 2 shows the transmittance spectra of selected polished samples before and after annealing. Before annealing (see Figure 2a), Al_2O_3-excess samples show low transmittance (below 50% at 1064 nm) and exhibits strong absorption at wavelength below 600 nm, which causes the red color of the Al_2O_3-excess sample (see Figure 1a). Transmittance of the ceramics also declines with the increase of Al_2O_3 in excess. Ceramics with transmittance ranging from 79% to 67% at 1064 nm can be obtained when the composition ranges from stoichiometric Nd:YAG to Y-2.0%. Transmittance

of the ceramics declines with the increase of Y_2O_3 in excess. Strong absorption at wavelength below 600 nm of Al_2O_3-excess samples can be reduced with the annealing treatment (see Figure 2b). Transmittance of ceramics with composition in between stoichiometric Nd:YAG and Y-2% is also improved especially in the wavelength ranging from 300 nm to 600 nm after the annealing process.

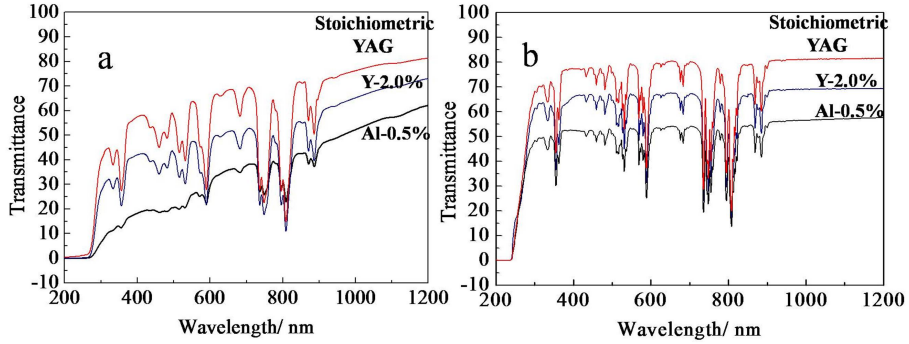

Figure 2. Transmittance spectra of sintered Nd:YAG samples with different composition (a) before annealing, (b) after annealing.

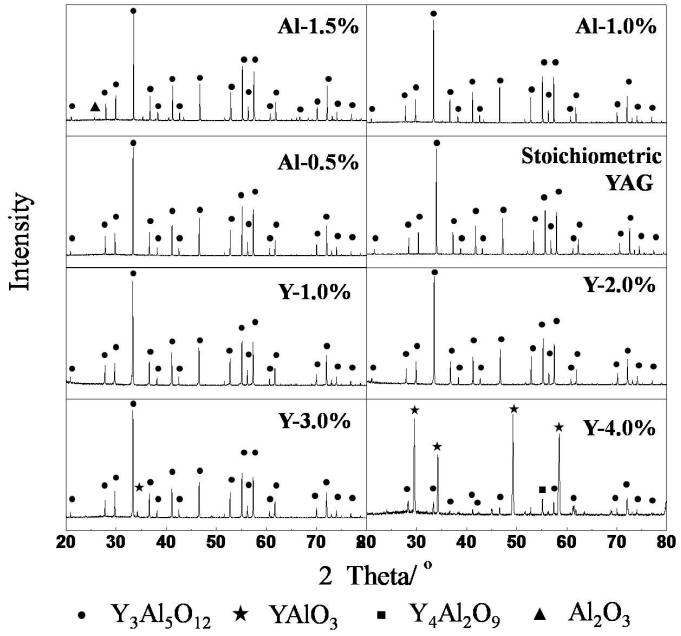

Figure 3. XRD pattern at room temperature for the sintered Nd:YAG samples with different composition.

Figure 3 shows the XRD patterns of different sintered samples at room temperature. Diffraction pattern of pure YAG (JCPDS no.33-40) is observed from the samples with composition ranging from Al-1.0% to Y-2.0%, no diffraction peaks of other compound is detected. However, diffraction peaks at 25.86°, 35.23°, etc. of

Al_2O_3 (JCPDS no.3-1033) is observed in sample with 1.5% excessive Al_2O_3, indicating that excessive constitution exist as second phase in the form of Al_2O_3. When Y_2O_3 is excessive for more than 2.0 at%, diffraction peaks of Y-rich compounds, such as $YAlO_3$ (JCPDS no.38-222), $Y_4Al_2O_9$ (JCPDS no.34-368), are detected. Those results also indicate that Y-rich compounds are more soluble in YAG crystalline structure than Al_2O_3 since the diffraction peaks of Y-rich compounds can only be detected when excessive Y_2O_3 is over 2% compared to that of Al_2O_3 (1%). However, we can see from Figure 3 that when excessive Y_2O_3 is over 2%, diffraction peaks of Y-rich compounds especially $YAlO_3$ show evident emergence. The reason can be attributed to the following formation mechanism of $YAlO_3$:

$$Y_2O_3 + Y_3Al_5O_{12} \longrightarrow 5YAlO_3$$

Excessive Y_2O_3 consumes $Y_3Al_5O_{12}$ at the same dosage while it generates $YAlO_3$ 5 times of its dosage. That also explains why Y_2O_3-excess samples transform from almost transparent to opaque in a relative narrow composition range (see Figure 1). Selected sintered samples (Al-1.5%, Stoichiometric Nd:YAG, Y-3.0%) was sent for inductively coupled plasma characterization and Rietveld refinement. The results are in good accord with our initial ingredient (see Figure S1, S2, Table S1 in the Supplementary Information). It indicates that all the starting materials were remain in the as prepared ceramics.

Table 1. Formation energies of O vacancy in different ceramic samples calculated by Maija M. Kuklja and Diffusion constant/ Diffusion activation energy reported by Isao Sakaguchi

Sample	Lowest formation energies of O vacancy[17]	Diffusion constant at 1673K [11]	Diffusion activation energy at 1673K [11]
Y_2O_3-excess YAG Ceramic	7.4 eV	7.7×10^{-11} m^2/s	223.9 kJ/mol
YAG	21.54 eV	4.3×10^{-8} m^2/s	304.1 kJ/mol
Al_2O_3-excess YAG Ceramic	5.7 eV	3.9 m^2/s	519.4 kJ/mol

Besides, the red color of the Al_2O_3-excess samples and the fact that it can be faded by annealing in oxygen atmosphere indicate that the red color can be attributed to the higher O vacancy generated during the vacuum sintering process in Al_2O_3-excess samples[13]. According to the reported investigation of the intrinsic

point defect formation in YAG (see Table 1) [11,14], excessive Al_2O_3 speeds up oxygen diffusion while excessive Y_2O_3 suppresses oxygen diffusion in YAG in vacuum. The formation energy of oxygen vacancy V_O in the Al_2O_3-excess YAG (5.7 eV) is much lower than that in the stoichiometric YAG (21.54 eV). It explains the higher concentration of O vacancy in Al_2O_3-excess samples.

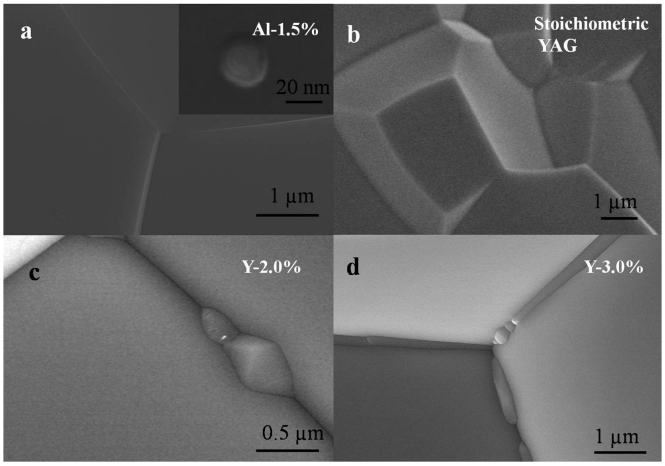

Figure 4. SEM micrographs showing the sintered Nd:YAG samples with different composition.

Figure 4 exhibits the SEM image of different samples. Sample Al-1.5% shows regular grains and clean grain boundaries (see Figure 4a). However, nanograins with scale around 20 nm embedded in YAG grain matrix can be found. Combined with XRD result of the Al_2O_3-excess samples, these nanoparticles embedded in YAG grain should be Al_2O_3 nanograins. This result is also consistent with our previous report about the existence of Al_2O_3 in Al_2O_3-excess YAG nanopowder [15]. Stoichiometric Nd:YAG ceramic obtains homogeneous grains and clean grain boundaries (see Figure 4b). In Y_2O_3-excess samples, small independent nanoparticles with scale around 30-100 nm can be observed at grain boundaries among YAG grains (see Figure 4c). With the increase of Y_2O_3 content, the number of nanoparticles at grain boundary increase, and connect together to form a continuous layer about 200 nm in thickness at the grain boundary between two neighboring grains in Sample Y-3.0% (see Figure 4d). According to the XRD result shown in Figure 3, nanograins observed at grain boundaries can be indexed as Y-rich compounds, $YAlO_3$ or $Y_4Al_2O_9$. The above results indicate that different nonstoichiometry in YAG ceramics can induce different microstructures with different co-existed second phases.

Figure 5 exhibit the HRTEM image of different samples. Nanograins with scale around 20-30 nm embedded in YAG grain matrix can be found in HRTEM image of Al-1.5% (see Figure 5a), lattice image of these nanograins can be indexed as Al_2O_3 according to its reciprocal lattice. Stoichiometric Nd:YAG ceramic obtains homogeneous grains and clean grain boundaries with clear lattice image (see Figure 5b). From Figure 5c, 5d, an area of different lattice image of a second phase can be found at the grain boundary between two YAG grains, and consistent $YAlO_3$ crystalline structure can be identified in Y-3.0% sample, which is consistent of the result shown in the XRD result and SEM observation.

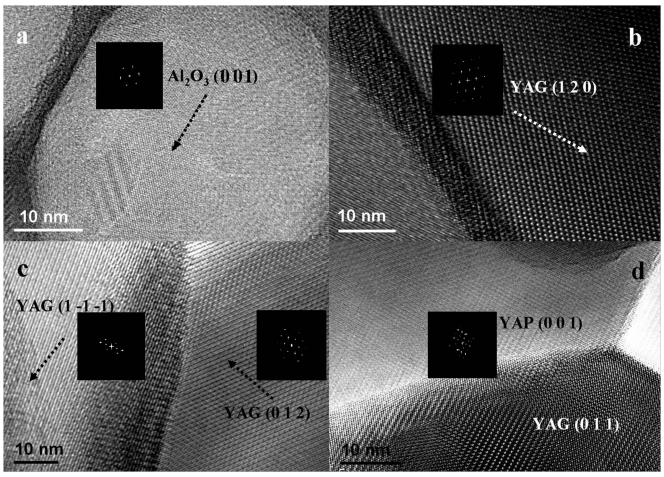

Figure 5. HRTEM micrographs showing the sintered Nd:YAG samples with different composition (a). Al-1.5%; (b). Stoichiometric YAG; (c). Y-2.0%; (d). Y-3.0%.

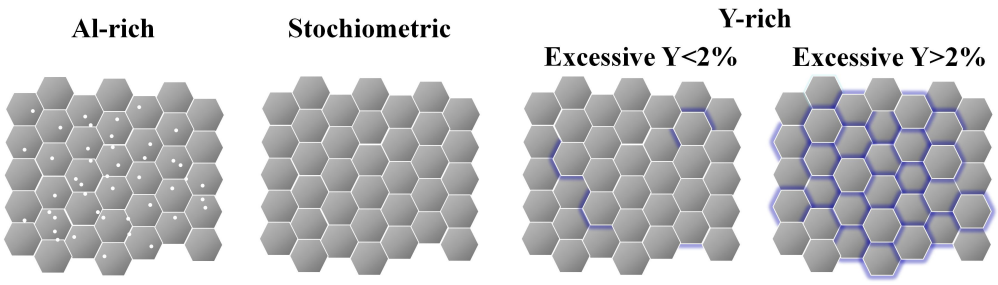

Figure 6. Schematic illustration of microstructure evolution of Nd:YAG with different composition deviation.

Based on the results above, schematic illustration of microstructure evolution of Nd:YAG with different composition deviation is shown in Figure 6. According to the phase diagram of the Y_2O_3-Al_2O_3 system, the solubility of Al_2O_3 in YAG is extremely low (<0.2%) compared to solubility of Y-rich compound in YAG (2% to 10%) [16]. It

indicates that a little amount of excess Al_2O_3 can induce Al_2O_3 nanograins in YAG grains, which causes the foggy appearance and low transmittance of Al_2O_3-excess sample. While little amount of Y_2O_3 will not induce second phase in as-synthesized YAG powder during the synthesis, and Y-rich Y-Al-O phase, such as $YAlO_3$, or $Y_4Al_2O_9$ at the boundary among YAG grains. In that case, considering the refractive indexes of Al_2O_3, YAG, YAP at 400 nm, which are 1.78, 1.86, 1.92[18-20], Al_2O_3 will causes much severer scattering and birefringence phenomenon of photons. That explains why Al_2O_3-excess sample obtains lower transparency than that of ceramics with relative low dosage of excessive Y_2O_3. However, with the increase of excessive Y_2O_3 content, nanoparticles at grain boundary will appear, quickly increase and connect together to form a continuous layer. That causes the Y_2O_3-excess samples transform from almost transparent to opaque in a relative narrow composition range.

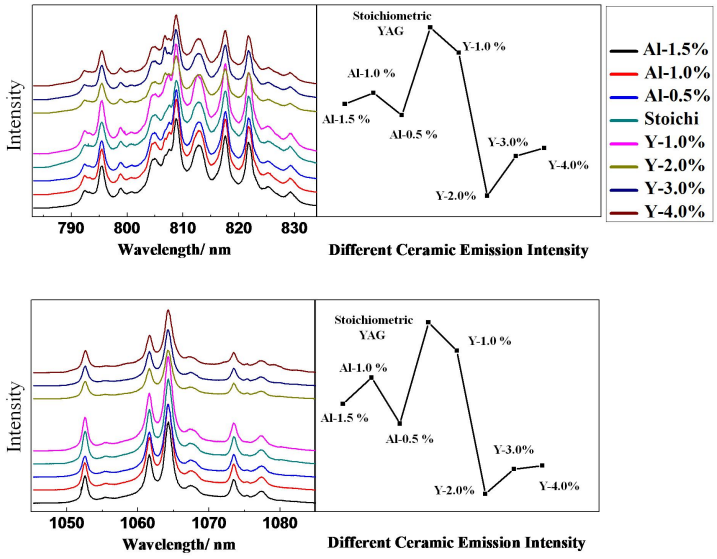

Figure 7. PL spectra of sintered Nd:YAG samples with different composition at 808 nm and 1064 nm.

Figure 7 shows the room temperature PL spectra of sintered ceramic samples with different composition around 808 nm and 1064 nm. Characteristic peaks of Nd ions from the transition $^2H_{9/2}/^4F_{5/2} \longrightarrow {}^4I_{9/2}$ at 792.43 nm, 795.38 nm, 798.86 nm, 804.72 nm, 807.53 nm, 808.76 nm, 812.82 nm, 817.57 nm, 821.80 nm, 825.41 nm, 829.20 nm and peaks from the transition $^4F_{3/2} \longrightarrow {}^4I_{11/2}$ at 1052.54 nm, 1061.64 nm, 1064.24 nm, 1067.52 nm, 1073.52 nm, and 1077.39 nm are observed in all samples.

PL spectra of Al_2O_3-excess and Y_2O_3-excess samples are almost the same as that of stoichiometric Nd:YAG ceramic. However, the emission intensity of Al_2O_3-excess and Y_2O_3-excess samples around 808 nm and 1064 nm are evidently weakened.

Figure 8 shows the room temperature time resolved PL spectra of sintered ceramic samples with different composition at 1064 nm. All decay curves appear to be similar and exhibit little difference before and after annealing. The calculated life time of this transition is around 205 μs, which is almost identical to the reported lifetime value of Nd:YAG ceramics (210 μs)[21], indicating that the composition deviation has little impact on the energy levels of Nd ions.

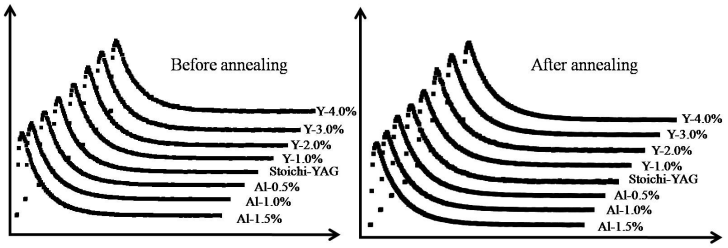

Figure 8. Time resolved spectra of Nd:YAG with different composition at 1064 nm.

Based on the results shown in Figure 7 and Figure 8, we can conclude that the declined emission intensity of Al_2O_3-excess and Y_2O_3-excess samples around 808 nm and 1064 nm is mainly caused by the existence of the second phases in non-stoichiometric samples. Loss of photons during its propagation in ceramic matrix with second phases will be much severe since non-cubic Al_2O_3, $YAlO_3$ and $Y_4Al_2O_9$ would form scattering centers and birefringence interfaces in cubic YAG medium. At the same time, the peak positions of PL spectra are not sensitive to composition deviation of the ceramics at this range. Electron configuration of Nd atom is $1s^2\ 2s^2\ 2p^6\ 3s^2\ 3p^6\ 3d^{10}\ 4s^2\ 4p^6\ 4d^{10}\ 4f^4\ 5s^2\ 5p^6\ 6s^2$. Different crystal fields usually have more significant effect on the outer layer of elctrons. 4f electrons locate in the inner shell of electron configuration of Nd atom. Shielding effect of $5s^2\ 5p^6\ 6s^2$ electrons will significantly weaken the effect of the crystal field. In this paper, composition deviation is proved to be an effective way to adjust ceramic microstructures. Different crystalline phases were observed. However, according to the explanation above, notable effect of different crystalline phases on the transition process of 4f electrons

was not detected. All emission spectra and decay curves around these two wavelengths appear to be similar. Although different crystalline phases have little effect on the transition process of 4f electrons, microstructure evolution of ceramics can evidently affect the photon transmission process. Therefore, the emission intensity of Al_2O_3-excess and Y_2O_3-excess samples around 808 nm and 1064 nm are evidently weakened due to the scattering centers and birefringence interfaces formed in those samples.

Conclusion

Transparent YAG ceramics can be obtained with its composition in between stoichiometric Nd:YAG and Y-2%. Excessive Al_2O_3 causes nanograins remaining in the YAG grain, while the Y-rich compound recrystallizes at the grain boundaries as the second phase because of relative higher solubility of Y-rich compound than Al_2O_3 in YAG crystalline structure. Spectra of non-stoichiometric samples are almost the same as that of stoichiometric Nd:YAG ceramic. Declined emission intensity of Al_2O_3-excess and Y_2O_3-excess samples around 808 nm and 1064 nm is mainly caused by the existence of the second phases. Results of this work can offer approach to optimize ceramic microstructures according to designed composition deviation and further deepen our understanding in the microstructure evolution process and mechanism of garnet ceramics.

Acknowledgements

This research was supported by NSFC (11404351, 51402317), Ningbo Municipal Nature Science Foundation (2014A610003, 2014A610014, 2014A610122). China Postdoctoral Science Foundation 2014M561801.

Reference

[1] J . E. Geusic, H. M. Marcos, and L. G. Van Uitert, Appl. Phys. Lett., 4(10), 182, 1964.

[2] G. de With, and H. J. A. van Dijk, Mater. Res., 19,1669, 1984.

[3] M. Selita, H. Haneda, T. Yanagitani, and S. Shirasaki, J. Appl. Phys., 67(1), 453, 1990.

[4] A. Ikesue, I. Furusato, and K. Kamata, J. Am. Ceram. Soc., 78(1), 225,1995.

[5] T. Yanagitani, H. Yagi, and M. Ichikawa, Japanese patent, 1998, 10-101333.

[6] T. Yanagitani, H. Yagi, and Y. Hiro, Japanese patent, 1998, 10-101411.

[7] J. R. Lu, K. Ueda, H. Yagi, T. Yanagitani, Y. Akiyama, and A. A. Kaminskii, J. Alloy Compd., 341(1-2), 220, 2001.

[8] A. Ikesue, T. Kinoshita, K. Kamata, and K. Yoshida, J. Am. Ceram. Soc., 78(4), 1033, 1995.

[9] T. Sekino, Y. Sogabe, Rev. Laser Eng., 21(8), 827, 1995.

[10] Dowes D., Industr. Laser Rev., Mar., 9, 1995.

[11] I. Sakaguchi, H. Haneda and J. Tanaka, J. Am. Ceram. Soc., 79(6), 1627, 1996.

[12] A. Ikesue, K. Kamata and K. Yoshida, J. Am. Ceram. Soc., 79(7), 1921, 1996.

[13] H. Haneda, Y. Miyazawa and S. Shirasaki., J. Cryst. Growth, 68, 581, 1984.

[14] Z. Li, B. Liu, J. M. Wang, L. C. Sun, J. Y. Wang and Y. C. Zhou, J. Am. Ceram. Soc., 95(11), 3628, 2012.

[15] Y. H. Sang, D. H. Yu, M. Avdeev, H. M. Qin, J. Y. Wang, H. Liu and Y. H. Lv, J. Solid State Chem., 192, 366, 2012.

[16] A. P. Patel, M. R. Levy, R. W. Grimes, R. M. Gaume, R. S. Feigelson, K. J. McClellan, and C. R. Stanek, Appl. Phys. Lett., 93, 191902, 2008.

[17] M. M. Kuklja and R. Pandey, J. Am. Ceram. Soc., 82 (10), 2881, 1999.

[18] SOPRA N&K Database.

[19] Handbook of Optics, 3rd edition, Vol. 4., McGraw-Hill, 2009.

[20] S. Baccaro, A. Cecilia, M. Montecchi, T. Malatesta, F. de Notaristefani,S. Torrioli and F. Vittori, Nucl. Instrum. Methods Phys. Res. A, 1998, 406, 479-485

[21] A. Ikesue, Y. L. Aung, T. Taira, T. Kamimura, K. Yoshida, and G. L. Messing, Annu. Rev. Mater. Res., 2006, 36, 397-429.

[22] J. Liu, L. Lin, J. Li, J. Liu, Y. Yuan, M. Ivanovc, M. Chen, B. L. Liu, L. Ge, T. F. Xie, H. M. K, Y. Shi, Y. B. Pan, J. K. Guo, Ceramics International, 2014, 40, 9841-9851.